Flavor decomposition of the nucleon electromagnetic form factors at low Q^{2}

I. A. Qattan, J. Arrington, and A. Alsaad

Phys. Rev. C **91**, 065203 — Published 19 June 2015

DOI: 10.1103/PhysRevC.91.065203

Flavor decomposition of the nucleon electromagnetic form factors at low Q^2

I. A. Qattan,[1] J. Arrington,[2] and A. Alsaad[3]

[1]*Khalifa University of Science, Technology and Research, Department of Applied Mathematics and Sciences, P.O. Box 127788, Abu Dhabi, UAE*
[2]*Physics Division, Argonne National Laboratory, Argonne, Illinois, 60439, USA*
[3]*Jordan University of Science and Technology, Department of Physical Sciences, P.O. Box 3030, Irbid 22110, Jordan*

(Dated: June 5, 2015)

Background The spatial distribution of charge and magnetization within the proton is encoded in the elastic form factors. These have been precisely measured in elastic electron scattering, and the combination of proton and neutron form factors allows for the separation of the up- and down-quark contributions.

Purpose In this work, we extract the proton and neutron form factors from world's data with an emphasis on precise new data covering the low-momentum region, which is sensitive to the large-scale structure of the nucleon. From these, we separate the up- and down-quark contributions to the proton form factors.

Method We combine cross section and polarization measurements of elastic electron-proton scattering to separate the proton form factors and two-photon exchange (TPE) contributions. We combine the proton form factors with parameterization of the neutron form factor data and uncertainties to separate the up- and down-quark contributions to the proton's charge and magnetic form factors.

Results The extracted TPE corrections are compared to previous phenomenological extractions, TPE calculations, and direct measurements from the comparison of electron and positron scattering. The flavor-separated form factors are extracted and compared to models of the nucleon structure.

Conclusions With the inclusion of the precise new data, the extracted TPE contributions show a clear change of sign at low Q^2, necessary to explain the high-Q^2 form factor discrepancy while being consistent with the known $Q^2 \to 0$ limit. We find that the new Mainz data yield a significantly different result for the proton magnetic form factor and its flavor-separated contributions. We also observe that the RMS radius of both the up- and down-quark distributions are smaller than the RMS charge radius of the proton.

PACS numbers: 25.30.Bf, 13.40.Gp, 14.20.Dh

I. INTRODUCTION

The electromagnetic form factors of the proton and neutron, $G_E^{(p,n)}$ and $G_M^{(p,n)}$, are fundamental quantities which provide information on the spatial distributions of charge and magnetization in nucleons. The form factors are measured using electron scattering where the incident electron scatters from a nucleon target through the exchange of a virtual photon which serves as the sole mediator of the electron-nucleon electromagnetic interaction. By increasing Q^2, the four-momentum squared of the virtual photon, the virtual photon becomes more sensitive to the small scale internal structure of the nucleon.

In electron scattering there are primarily two methods used to extract the proton form factors. The first is the Rosenbluth or Longitudinal-Transverse (LT) separation method [1], which uses measurements of the unpolarized cross section, and the second is the polarization transfer or polarized target (PT) method [2], which requires measurement of the spin-dependent cross section. A significant difference is observed between LT and PT extractions of the proton form factors [3, 4], which is currently believed to be the results of larger-than-expected two-photon exchange (TPE) contributions [5, 6].

In this paper, we extract the proton form factors from a combined analysis of LT and PT measurements, accounting for TPE contributions following the approach of Ref. [7], but with an emphasis on recent low-Q^2 data. The combined analysis allows us to extract the TPE contribution to the e-p elastic cross section, which we compare to other phenomenological extractions and to direct calculations of TPE effects meant to be valid in the lower Q^2 regime, as well as to recent direct measurements of TPE contributions from the comparison of electron-proton and positron-proton elastic scattering [8, 9].

With the inclusion of neutron form factor measurements, we separate the nucleon form factors into their up-quark and down-quark contributions [10, 11]. New cross section and polarization measurements at low Q^2 allow for a more detailed examination of the flavor-separated form factors in the region sensitive to the large-distance behavior of the proton charge and magnetization distributions. We compare these results to previous extractions, as well as to models of the up- and down-quark contributions to the proton form factors.

II. OVERVIEW OF THE METHODS

A. Rosenbluth Separation Method

In the Rosenbluth separation method, the reduced cross section σ_R for elastic e-p scattering in the Born or one-photon exchange (OPE) approximation is:

$$\sigma_R = \left(G_M^p(Q^2)\right)^2 + \frac{\varepsilon}{\tau}\left(G_E^p(Q^2)\right)^2, \qquad (1)$$

where $\tau = Q^2/4M_p^2$, M_p is the mass of the proton, and ε is the virtual photon longitudinal polarization parameter, defined as $\varepsilon^{-1} = \left[1 + 2(1+\tau)\tan^2(\frac{\theta_e}{2})\right]$, where θ_e is the scattering angle of the electron. For a fixed Q^2 value, the reduced cross section σ_R is measured at several ε points, and a linear fit of σ_R to ε gives $(G_M^p)^2$ as the intercept and $(G_E^p)^2/\tau$ as the slope.

By assuming isospin and charge symmetry and neglecting strange quarks contribution, the nucleon form factors can be expressed in terms of the up- and down-quark contributions [12, 13]

$$G_{E,M}^p = \frac{2}{3}G_{E,M}^u - \frac{1}{3}G_{E,M}^d,$$
$$G_{E,M}^n = \frac{2}{3}G_{E,M}^d - \frac{1}{3}G_{E,M}^u, \quad (2)$$

where in this convention $G_{E,M}^u$ represents the contribution from the up-quark distribution in the proton and the down-quark distribution in the neutron.

Solving for $G_{E,M}^u$ and $G_{E,M}^d$ from Eq. (2) above, we get the following expression for the up- and down-quark contribution to the proton form factors

$$G_{E,M}^u = 2G_{E,M}^p + G_{E,M}^n, \quad G_{E,M}^d = G_{E,M}^p + 2G_{E,M}^n. \quad (3)$$

In the limit $Q^2 = 0$, this yields $G_E^u = 2, G_E^d = 1, G_M^u = (2\mu_p + \mu_n) = 3.67\mu_N$, and $G_M^d = (\mu_p + 2\mu_n) = -1.03\mu_N$, where μ_N is the nuclear magneton.

B. Recoil Polarization Measurements

In the recoil polarization method, a beam of longitudinally polarized electrons scatters elastically from unpolarized proton target. The electrons transfer their polarization to the unpolarized protons. By simultaneously measuring the transverse, P_t, and longitudinal, P_l, polarization components of the recoil proton, one can determine the ratio $\mu_p G_E^p/G_M^p$ in the OPE [2, 14, 15]:

$$R = \frac{\mu_p G_E^p}{G_M^p} = -\frac{P_t}{P_l}\frac{(E+E')}{2M_p}\tan(\frac{\theta_e}{2}), \quad (4)$$

where E and E' are the initial and final energy of the incident electron, respectively. The ratio can be extracted in a similar fashion using polarized beams and targets by measuring the asymmetry for two different spin directions [3, 4].

The two methods yield strikingly different results, with values of $\mu_p G_E^p/G_M^p$ differing almost by a factor of three at high Q^2. In the LT separation method, the ratio shows approximate form factor scaling, $\mu_p G_E^p/G_M^p \approx 1$, albeit with large uncertainties at high Q^2 values. The recoil polarization method yields a ratio that decreases roughly linearly with increasing Q^2, with some hint of flattening out above 5 $(\mathrm{GeV/c})^2$.

C. Two-Photon Exchange Contributions

To reconcile these measurements, several studies suggested that missing higher order radiative corrections to the electron-proton elastic scattering cross sections, in particular two-photon exchange (TPE) diagrams, may explain the discrepancy [16–18]. The role of TPE effects was studied extensively both theoretically [19–24] and phenomenologically [16, 25–32]. Most calculations suggested that the TPE corrections are relatively small, but have a significant angular dependence which mimics the effect of a larger value of G_E^p. Detailed reviews of the role of the TPE effect in electron-proton scattering can be found in [5, 6].

Experimentally, several measurements were performed to verify the discrepancy [33, 34] and to try and measure or constrain TPE contributions. Precise examinations of the ε dependence of σ_R [25, 26, 28] found no deviation from the linear behavior predicted in the OPE approximation. Another measurement was performed to look for TPE effects by extracting $\mu_p G_E^p/G_M^p$ at fixed Q^2 as a function of scattering angle [35]. In the Born approximation, the result should be independent of scattering angle, and no deviation from the OPE prediction was observed.

Based on the observations above, it is possible to try and extract the TPE contributions based on the observed discrepancy between the LT and PT results. Assuming that the TPE contributions are linear in ε and that the PT results do not depend on ε, and knowing that the TPE contribution must vanish in the forward limit ($\varepsilon \to 1$) [28, 36], it is possible to extract the TPE contribution to the unpolarized cross section in a combined analysis of LT and PT data [7, 16, 27–29, 37]. Where polarization data exist as a function of ε, it is possible to attempt to extract the TPE amplitudes with fewer assumptions [30, 38], though with relatively large uncertainties.

The most direct technique for measuring TPE is the comparison of electron-proton and positron-proton scattering. The leading TPE contribution comes from the interference of the OPE and TPE amplitudes, and so has the opposite sign for positron and electron scattering. The only other first-order radiative correction which depends on the lepton sign is the interference between diagrams with Bremsstrahlung from the electron and proton, and this contribution is generally small. Thus, after correcting the measured ratio for the Bremsstrahlung interference term, the comparison of positron and electron scattering allows for the most direct measurement of TPE contributions.

The ratio $R_{e^+e^-}(\varepsilon, Q^2)$ is defined as

$$R_{e^+e^-}^{\mathrm{raw}}(\varepsilon, Q^2) = \frac{\sigma(e^+p \ \to e^+p)}{\sigma(e^-p \ \to e^-p)}. \quad (5)$$

After correcting for the electron-proton Bremsstrahlung interference term and the conventional charge-independent radiative corrections, the cross section

ratio $R_{e^+e^-}$ reduces to:

$$R_{e^+e^-}(\varepsilon, Q^2) = \frac{1-\delta_{2\gamma}}{1+\delta_{2\gamma}} \approx 1 - 2\delta_{2\gamma}, \quad (6)$$

where $\delta_{2\gamma}$ is the fractional TPE correction for electron-proton scattering. Until recently, there was only limited evidence for any non-zero TPE contribution from such comparisons [39], as data were limited to low Q^2 or large ε, where the TPE contributions appear to be small. In addition, the details of the radiative corrections applied to these earlier measurements are not always available, and it is not clear if the charge-even corrections were applied in all cases. New measurements [8, 9] have found more significant indications of TPE contributions at low ε and moderate Q^2, with the ratio of positron-proton to electron-proton scattering larger than unity. This is consistent with a variety of TPE calculations which include the effect of hadronic structure [20, 24, 40, 41] in somewhat different approximations, but has the opposite sign compared to the low-Q^2 (or high proton mass) limit [42] and finite-Q^2 calculations for a point-proton [6].

D. Extraction of the Form Factors and TPE

To extract the proton form factors, we assume TPE contributions to the polarization data are negligible and account for the contribution to σ_R by adding the real function $F(\varepsilon, Q^2)$ to the Born reduced cross section:

$$\sigma_R = \left(G_M^p\right)^2\left[1 + \frac{\varepsilon}{\tau}\frac{R^2}{\mu_p^2}\right] + F(\varepsilon, Q^2), \quad (7)$$

where $R = \mu_p G_E^p / G_M^p$ is the recoil polarization ratio.

We recently extracted the proton form factors and the TPE correction $a(Q^2)$ for large Q^2 values [7, 11] using the world data on σ_R from Refs. [33, 34, 43–48]. The form factors were extracted based on the parametrization from Borisyuk and Kobushkin (BK parametrization) [32], where σ_R is expressed in the following form

$$\sigma_R = \left(G_M^p\right)^2\left[1 + \frac{\varepsilon}{\tau}\frac{R^2}{\mu_p^2}\right] + 2a(Q^2)(1-\varepsilon)\left(G_M^p\right)^2. \quad (8)$$

This form accounts for the experimental and theoretical constraints presented in Sec. II C. The value for the ratio $R = \mu_p G_E^p / G_M^p$ is taken from a parameterization of the recoil polarization data, for which we assume there is no TPE contribution. In the analysis of Refs. [7, 11], the linear parameterization of R and its uncertainties from Ref. [49] was used. An additional uncertainty was applied in the analysis of Ref. [11] to provide more realistic uncertainties at lower Q^2, but this was not included in Ref. [7].

In this work, we extend the analysis of Ref. [11] to lower Q^2 values by including data from new, high-precision cross section measurements, and by improving the parameterization of R and its uncertainty from polarization measurements at both low and high Q^2 values. Taking the recoil-polarization and polarized-target results from Refs. [50–62], we parameterize the data with a simple inverse polynomial and find that the form factor ratio is well parameterized as:

$$R = \frac{1}{1 + 0.1430Q^2 - 0.0086Q^4 + 0.0072Q^6}. \quad (9)$$

The reduced χ^2 of the fit is relatively large (~ 1.5) driven by the scatter of the low Q^2 data. The reduced χ^2 is 1.15 if a handful of these data points (the three data points with $R > 1.0$ from BLAST [60] and the two lowest Q^2 points from Ref. [52]) are removed, however, the central fit is essentially unchanged and does not improve significantlly if the number of fit parameters is increased. Therefore, we conclude that the large reduced χ^2 is driven by the tension between the different data seta, rather than a limitation of the fit function. For the final fit, we do not exclude any of the data sets; as this was done only to examine the cause of the large reduced χ^2 value of the fit. We examine the uncertainties of the data as a function of Q^2 and based on a simple parameterization of this we take the fit uncertainty to be: $\delta_R^2(Q^2) = (0.006)^2 + (0.015\ln(1+Q^2))^2$, with Q^2 in $(\mathrm{GeV/c})^2$.

An argument could be made that the uncertainty might be below 0.6% for the low Q^2 values, especially as we approach $Q^2 = 0$ where the ratio is known. However, TPE calculations on the recoil-polarization ratio show effects that can be up to 0.5% [20] at low Q^2. Because we neglect TPE corrections to the polarization measurements, the uncertainties should be large enough to account for this. Figure 1 shows our new global fit to the world data on the recoil-polarization ratio $\mu_p G_E^p / G_M^p$ along with the fit's uncertainty bands.

III. RESULTS

A. Form Factors and TPE Contributions

We extract the form factors and the TPE contributions using Eq. (8), following the procedure of Ref. [11]. We obtain the value for R and its uncertainty from the new parameterization presented in Eq. (9). For most cross section data sets, measurements are available at fixed Q^2 over a range of ε values, allowing for the extraction of $a(Q^2)$ from Eq. (8). If the data are not at exactly the same Q^2, in particular for the data of Ref. [37], data in a narrow Q^2 range (with a spread in Q^2 that is typically well below 1%) are selected and corrected to a fixed Q^2 value using the form factor parameterization of Ref. [63]. The cross section data sets included are those used in Ref. [11] along with the addition of low-Q^2 data from Refs. [37, 43].

Figure 2 shows the extracted proton form factors from this work; these form factors and the TPE contribution are included in the online Supplemental Mate-

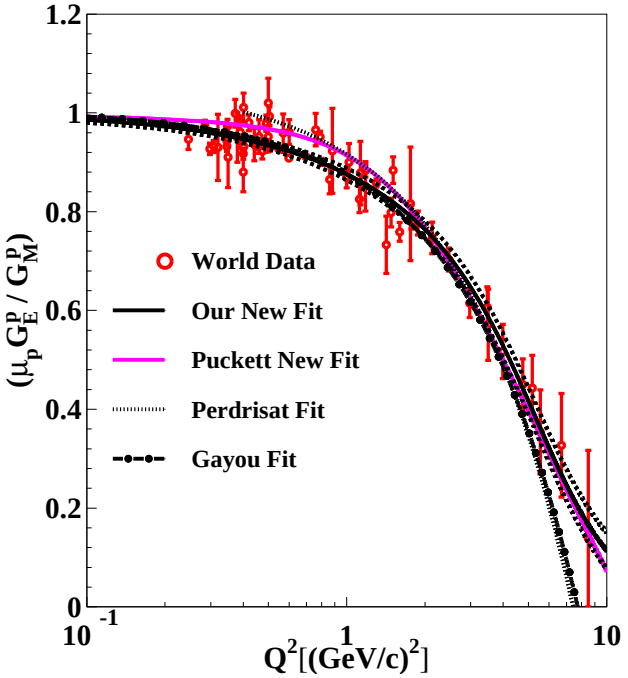

FIG. 1: (Color online) The world data on the recoil-polarization ratio $\mu_p G_E^p/G_M^p$ from Refs. [50–62] (open red circles) along with our new fit (solid black line) and its uncertainty bands (dashed black lines) and previous fits from Refs. [51] (solid magenta line), [4] (dotted black line), and [49] (dashed-dotted black line).

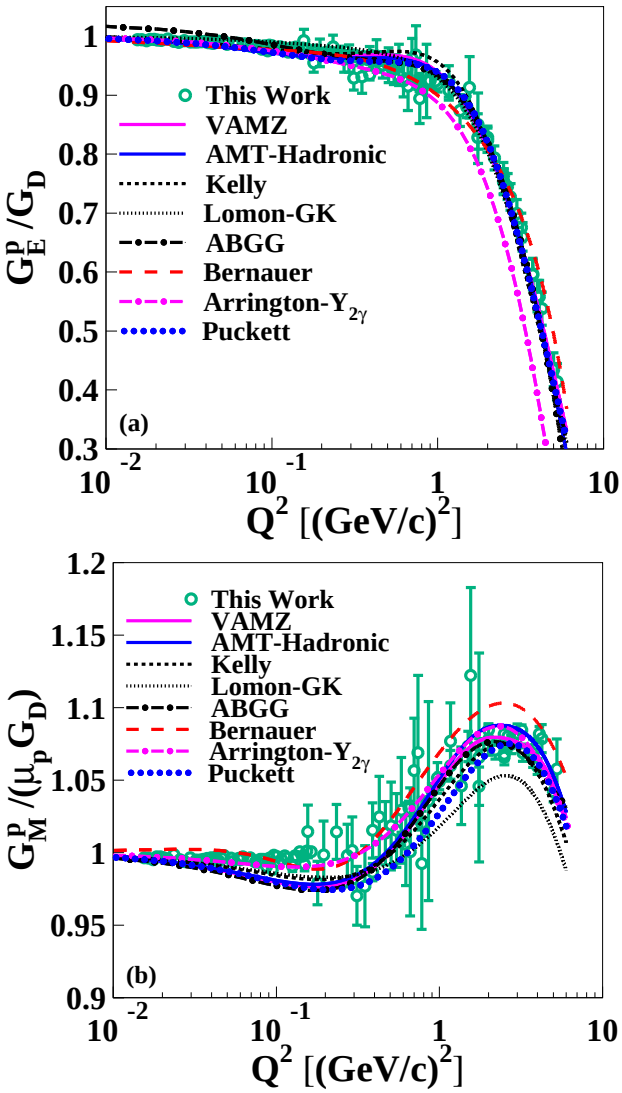

FIG. 2: (Color online) G_E^p/G_D (top) and $G_M^p/(\mu_p G_D)$ (bottom) as obtained using the BK parametrization from the data of Refs. [33, 34, 37, 43–48] (open dark-green circles). In addition, we compare our results to extractions from several previous TPE calculations and phenomenological fits: AMT [63] (solid blue line), VAMZ [65] (solid magenta line), Kelly [66] (short-dashed black line), Lomon-GK [67] (dotted black line), ABGG [68] (dashed-dotted black line), Bernauer [37] (long-dashed red line), Arrington $Y_{2\gamma}$ [29] (dashed-dotted magenta line), and Puckett (large-dotted blue line) (the fit labeled "new" in Ref. [51]).

rial [64]. We also show the form factors as extracted after applying hadronic TPE calculations, labeled "AMT-Hadronic" [63] and "VAMZ" Ref. [65]. In addition, we show fits to the form factors from previous phenomenological analyses: "Kelly" [66], "Lomon-GK" [67], "ABGG" [68], "Bernauer" [37], "Arrington-$Y_{2\gamma}$" [29], and "Puckett" [51].

While extractions using calculated TPE corrections and phenomenological-based fits are in reasonably good agreement, extractions which combine cross section and polarization results but do not allow for an explicit TPE correction, in particular the Kelly and Lomon extractions, tend to have larger differences. The "Arrington-$Y_{2\gamma}$" fit is very different at large Q^2 because it is the only analysis that allows for TPE contributions to the recoil polarization data, though the extraction of these terms is extremely model dependent.

At low Q^2, our extraction of G_M^p is significantly above most previous fits. This reflects the discrepancy between the recent Mainz data which yields values of G_M^p which are systematically 2–5% larger than previous world's data [37]. At low Q^2, this corresponds to only a small difference in the cross section at large scattering angle, but for the larger Q^2 values of the Mainz experiment, this corresponds to a significant difference in the measured cross sections. Note that except for the Bernauer result, most of the previous phenomenological extractions of the form factors and TPE contributions were focused on large Q^2 values, and so did not always worry about how well the parameterizations of R reproduced low Q^2 data.

Figure 3 shows the TPE term $a(Q^2)$ extracted from this work. We also show parameterizations of $a(Q^2)$ from the TPE hadronic calculations of Ref. [20] (BMT) and Ref. [63] (AMT), which adds and additional phenomenological TPE contribution at higher Q^2, and from previous phenomenological extractions [7, 37]. At high-Q^2 values, the TPE term is consistent with our previous extraction and shows an increase in magnitude with in-

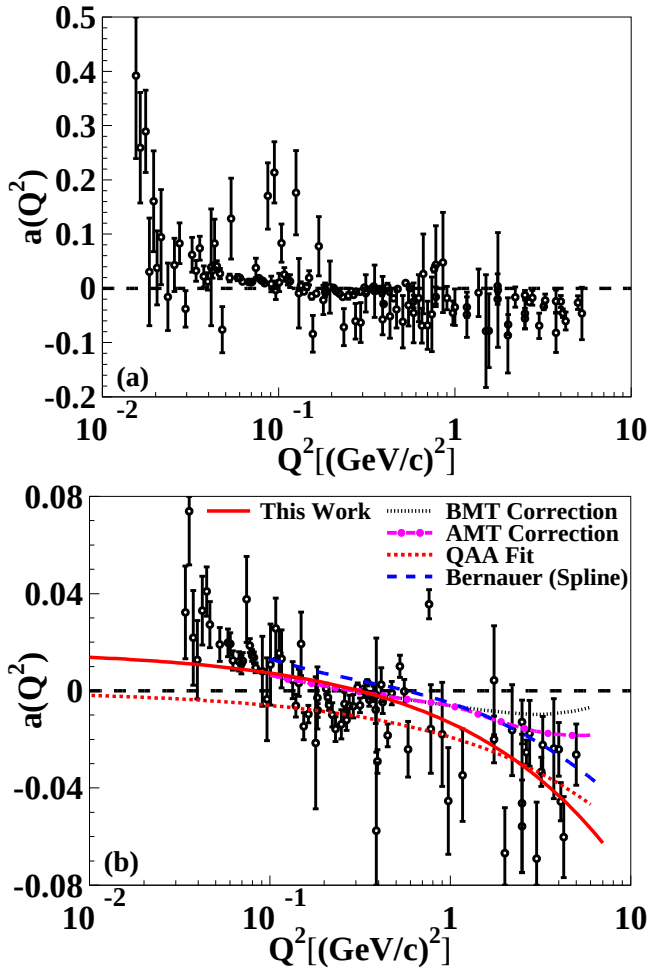

FIG. 3: (Color online) The TPE term $a(Q^2)$ as obtained using the BK parametrization from the data of Refs. [33, 34, 37, 43–48] (open black circles). Also shown are a simple parameterization of our results (solid red line) and curves representing $a(Q^2)$ as determined in previous analyses from Refs. [20] (dotted black line), [63] (dashed-dotted magenta line), [7] (short-dashed red line), and [37] (large-dashed blue line). The bottom plot is on a smaller vertical scale, excluding points with uncertainties above $\delta a = 0.03$ for clarity, although they are included in our fit. Note that we do not show extractions of $a(Q^2)$ for the calculations or extraction of Ref. [37] at very low Q^2, as the ε dependence is quite different in our parameterization when the cross sections are dominated by the charge form factor (see text).

creasing Q^2. The previous extraction [7] was not well constrained at low Q^2, with cross section data limited to $Q^2 \geq 0.39$ and a parameterization [49] of the polarization data that was not well constrained at low Q^2. So below $Q^2 \approx 1$ (GeV/c)^2, the behavior was driven by the fitting function which took $a(Q^2)$ proportional to $\sqrt{Q^2}$. In the present work, the inclusion of the Mainz data and low Q^2 polarization provide meaningful uncertainties for $a(Q^2)$ below $Q^2 = 1$ (GeV/c)^2 and show a change in sign at low Q^2, as seen in previous low-Q^2 TPE calculations [20, 32, 41, 69]. A similar extraction using neural networks was presented in Ref. [70], including a discussion of minimizing and evaluating the model dependence. However, the analysis did not include the new low Q^2 data we focus on in the present work.

While the values of $a(Q^2)$ extracted from Mainz data show hints of oscillatory behavior below $Q^2 = 0.3$ GeV^2, the uncertainties in the extracted TPE contribution are an underestimate of the true uncertainties. The quoted uncertainties on the individual cross sections do not include correlated systematic effects, which are a significant contribution to the total uncertainty in their final form factor parameterization, and we do not account for any residual uncertainty in the normalization of the data subsets which are fit as part of the global analysis [37]. So while this oscillatory behavior seems significant compared to the uncertainties that are shown, these uncertainties are incomplete and this cannot be taken as meaningful evidence for such structure. We fit to the Q^2 dependence of the extracted TPE contributions, adding an additional uncertainty, $da = 0.01$, to each point to help offset the impact of the underestimated uncertainties in our extraction from the Mainz data. Fitting the extracted $a(Q^2)$ values to a simple two parameter function yields $a(Q^2) = 0.016 - 0.030\sqrt{Q^2}$, with Q^2 in (GeV/c)^2. We do not quote a reduced χ^2 value on our fit as this would not be meaningful given that we do not have a complete evaluation of the uncertainties for $a(Q^2)$ from the Mainz data. Note that for our parameterization of TPE contributions, $F(Q^2,\varepsilon)/(G_M^p)^2$ is a linear function in ε, while the $Q^2 \to 0$ limit [6, 42] is more nearly linear when taken as a ratio to the reduced cross section, $(G_M^p)^2 + (\varepsilon/\tau)(G_E^p)^2$, and so the behavior at small Q^2, where $1/\tau$ becomes large, is very different. This can be seen more clearly in examining the ε dependence of the TPE contributions at very low Q^2, as shown in Fig. 4.

B. Ratio of Positron-Proton to Electron-Proton Elastic Scattering Cross Sections $R_{e^+e^-}$

From the TPE contributions extracted based on the parameterization of Eq. (8), the corrected ratio of positron-to-electron scattering cross sections is

$$R_{e^+e^-}(\varepsilon, Q^2) = \frac{1-\delta_{2\gamma}}{1+\delta_{2\gamma}} \approx 1 - \frac{4a(Q^2)(1-\varepsilon)}{(1+\frac{\varepsilon R^2}{\tau\mu_p^2})}. \quad (10)$$

Figure 4 shows the ratio $R_{e^+e^-}$ as a function of ε extracted for a range of Q^2 values. The solid red curve represents the ratio from our new parameterization of $a(Q^2)$, and the others show the results of TPE hadronic calculations from Refs. [20, 63] and several phenomenological fits from Refs. [7, 29, 37, 68]. The data points are world data on the ratio $R_{e^+e^-}$ from Refs. [8, 9, 71–80]. Two recent measurements [8, 9] have provided significantly more precise measurements at $Q^2 \approx 1.0$ and 1.5 (GeV/c)^2, providing evidence for non-zero TPE at larger Q^2 values and a change of sign from the exact calculation at $Q^2 = 0$, consistent with what we observe. Our

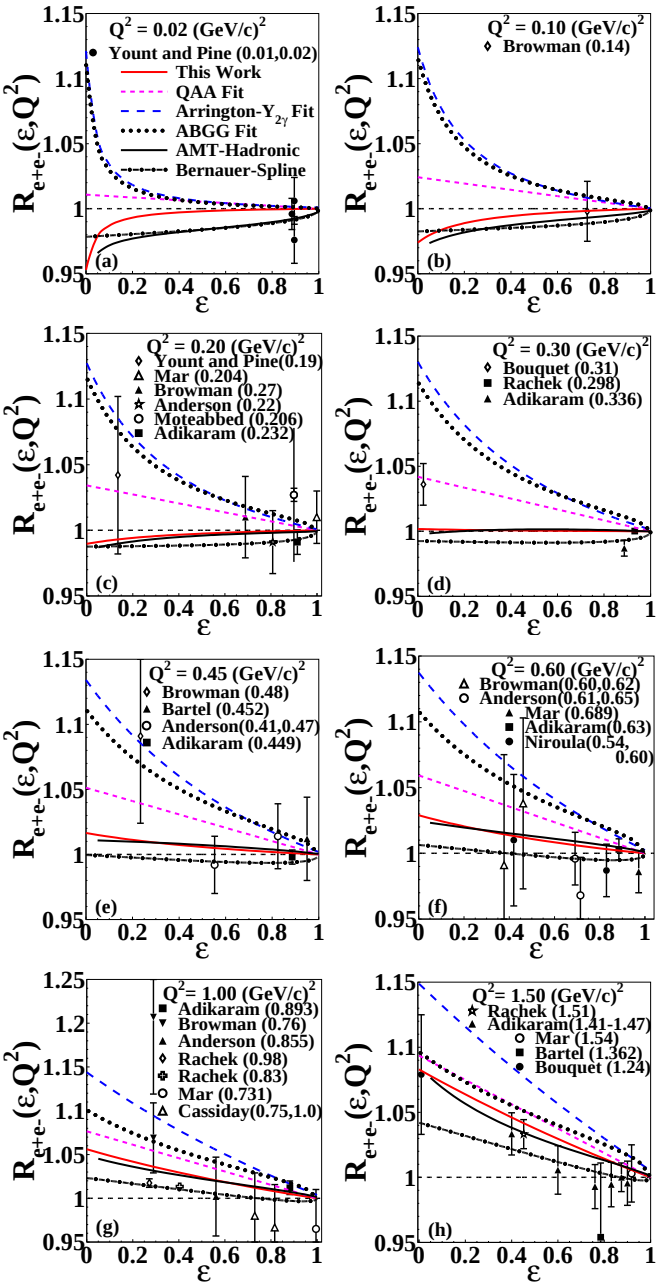

FIG. 4: (Color online) The ratio $R_{e^+e^-}(\varepsilon, Q^2)$ as determined from our parameterization of $a(Q^2)$ at the Q^2 value listed in the figure (solid red line). The other curves show previous calculations [63] (solid black line) or phenomenological extractions from Refs. [7] (short-dashed magenta line), [29] (long-dashed blue line), [68] (large-dotted black line), and [37] (dashed-dotted black line). The data points are direct measurements of $R_{e^+e^-}$ [8, 9, 71–80]. For the world data, the measurement and Q^2 value(s) in (GeV/c)^2 are given.

results are slightly larger than the direct measurements at 1 (GeV/c)^2 from Ref. [9], but otherwise in very good quantitative agreement with existing data.

Note that parameterizations where the TPE contribution is similar to that of Eq. (8), i.e. a linear function times $(G_M^p)^2$, the low Q^2 results for $R_{e^+e^-}$ will have a strong non-linear behavior. The TPE contribution relative to $(G_M^p)^2$ is linear, but $(G_E^p)^2$ dominates the cross section at very low Q^2 except for $\varepsilon \to 0$, strongly suppressing TPE as a fractional contribution as one moves away from $\varepsilon = 0$. This could be fixed by modifying the functional form, e.g. using a linear function in ε times the full reduced cross section [37]. However, because the results are similar everywhere except at very low Q^2, where there is little data, we consider this parameterization sufficient for the present analysis.

C. Flavor Separation of the Nucleon Form Factors

Examinations of the flavor-separated form factors of the nucleon focusing on high Q^2 [10, 11] have provided several interesting observations. Below we summarize some of the main conclusions from these analyses:

(1) The down-quark contributions to Dirac, F_1, and Pauli, F_2, form factors deviate from the expected $1/Q^4$ scaling [10], with small differences between the Q^2 dependence in F_1 and F_2 for both the up- and down-quark contributions.

(2) The up- and down-quark yield very different contributions [11] to G_E/G_M and F_2/F_1. The strong linear falloff with Q^2 in the ratio G_E^p/G_M^p is not seen in either the up- or down-quark contributions, but mainly arises due to a cancellation between a weaker Q^2 dependence for the up-quark and a negative but relatively Q^2-independent contribution from the down-quark.

(3) The more recent analysis [11] shows some differences from the original work by Cates *et al.* [10], referred to as "CJRW" throughout the text. The difference are associated with the approximations made in the CJRW analysis, which neglected TPE effects and included only the uncertainty associated with the neutron charge form factor. The treatment of TPE contributions yields small but clear differences, mainly at lower Q^2 values, up to ≈ 1.5 (GeV/c)^2, while the addition of uncertainties associated with TPE and all of the form factors yields somewhat larger uncertainties in most form factors, and provides an estimate for the uncertainties in the magnetic form factors absent in the CJRW analysis.

Figures 5 and 6 show the flavor-separated form factors extracted from this work; the extracted values are included in the online Supplemental Material [64]. The updated parameterization of the polarization-transfer measurements of $\mu_p G_E^p/G_M^p$ yields a small difference in the data above 5 (GeV/c)^2, but it is always a factor of 2-3 below the quoted uncertainties. Note that because the CJRW analysis includes only the uncertainties from G_E^n, the flavor-separated extraction of G_M is quoted without uncertainty. In our analysis, uncertainties are included for all form factors, but we use a parameterization for the uncertainty on G_E^n and G_M^n, taken from Ref. [11]. Be-

cause of this, cases where the uncertainty is dominated by neutron data yield points with large error bars but small scatter between points, as only the proton uncertainties are independent for each Q^2 values.

The results are compared to the original CJRW results and two recent extractions of the nucleon elastic form factors which apply calculated TPE contributions [63, 65]. Also shown are calculations based on dressed-quarks contribution within the frame work of Dyson-Schwinger equation "DSE" from Ref. [81], pion-cloud relativistic constituent quark model "PC-RCQM" from Ref. [82], relativistic constituent quark model whose hyperfine interaction is derived from Goldstone-boson exchange "GBE-RCQM" from Ref. [83, 84], and generalized parton distributions with incorporated Regge contribution that apply diquark models "GPD" from Ref. [85].

We start by examining the contributions to G_E^p. The down-quark contribution is much smaller than the up-quark contribution at all Q^2 values. Up to $Q^2 \approx 1$ (GeV/c)^2, both G_E^d/G_D and G_E^u/G_D increase with Q^2, deviating noticeably from the dipole form at $Q^2 \approx 0.10$ (GeV/c)^2 and $Q^2 \approx 0.40$ (GeV/c)^2, respectively. At higher Q^2 values, G_E^u/G_D decreases rapidly while G_E^d/G_D continues to increase, leading to the significant falloff in G_E^p/G_D after applying the charge weighting of the up- and down-quark contributions. While most of the calculations give a reasonable qualitative description of the data, all showing a rise and then fall of both G_E^d/G_D and G_E^u/G_D with increasing Q^2 values, the AMT-Hadronic and VAMZ parameterizations, as well as the GPD model, which also fits to the measured form factors, provide the best description of the data.

This work allows for a more detailed examination of the low-Q^2 region, which is sensitive to the RMS radius of the up- and down-quark distributions. At very low Q^2 values, G_E^u is consistent with the dipole fit, while G_E^d falls less slowly than the dipole, yielding an increase in the ratio G_E^d/G_D. The proton RMS charge radius as determined from electron scattering is $r_E \approx 0.88$ fm [37, 59]. The dipole form corresponds to an RMS radius of 0.811 fm, suggesting an RMS radius of approximately 0.81 fm for the up-quark distribution and below 0.81 fm for the down quarks. This gives $r_d < r_u < r_p$ for the charge radii, i.e. both the up- and down-quark distributions are more localized than the overall proton charge distribution, due to cancellation of the up- and down-quark contributions in the total proton charge distribution. Note that while the proton charge radius as extracted from muonic hydrogen measurements [86, 87] yield $r_E \approx 0.84$ fm, it is more natural to compare scattering results of the proton and flavor-separated contributions, although the up- and down-quark radii are also smaller than muonic hydrogen charge radius.

For G_M^p, the up-quark contribution is again dominant, even more so than for the charge form factor. Our results are in relatively good agreement with the CJRW analysis for Q^2 above 2 (GeV/c)^2, though with a small offset associated with TPE. For $Q^2 \lesssim 1$ (GeV/c)^2, we

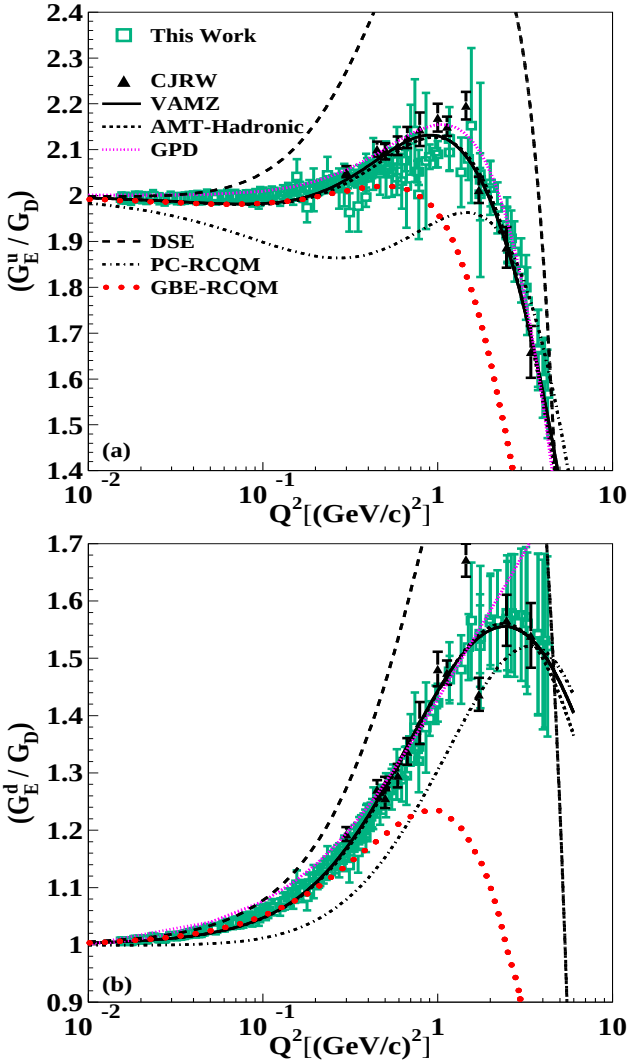

FIG. 5: (Color online) (G_E^u/G_D) (top) and (G_E^d/G_D) (bottom) as a function of Q^2 from the data of Refs. [33, 34, 37, 43–48] (open dark-green squares). Also shown the CJRW extractions [10] (solid black triangles), the AMT-Hadronic [63] (short-dashed black line) and VAMZ [65] (solid black line) fits, and the values from the GPD [85] (dotted magenta line), DSE [81] (long-dashed black line), PC-RCQM [82] (dashed-dotted black line), and GBE-RCQM [83, 84] (large-dotted red line) models. Note that for the proton, the up- and down-quark contributions have weighting factors of 2/3 and -1/3 (Eq. (2)).

find noticeably larger values for both the up- and down-quark contributions to the magnetic form factor. This difference comes from the Mainz data which yields values of G_M^p which are systematically larger than previous world's data, as seen in Fig. 2. Thus, it is not surprising that there is an inconsistency between the extraction from these data and other measurements, in particular for the up-quark contribution. For both the flavor-separated charge and magnetic form factors, the global fits [63, 65] describe the data (excluding the results from the Mainz measurement) well. The models with many

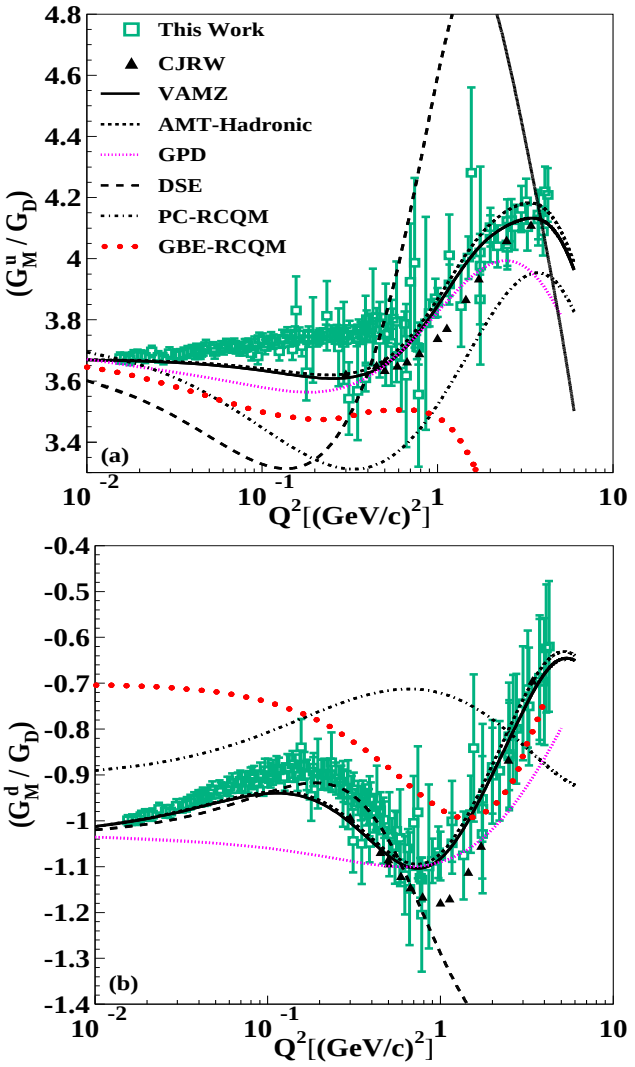

FIG. 6: (Color online) (G_M^u/G_D) (top) and (G_M^d/G_D) (bottom) as a function of Q^2 from the data of Refs. [33, 34, 37, 43–48] (open dark-green squares). Also shown the CJRW extractions [10] (solid black triangles), the AMT-Hadronic [63] (short-dashed black line) and VAMZ [65] (solid black line) fits, and the values from the GPD [85] (dotted magenta line), DSE [81] (long-dashed black line), PC-RCQM [82] (dashed-dotted black line), and GBE-RCQM [83, 84] (large-dotted red line) models. Note that for the proton, the up- and down-quark contributions have weighting factors of 2/3 and -1/3 (Eq. (2)).

free parameters [82, 85] tend to do a better job than the models with few or no parameters adjusted to match the form factor data [81, 84], although the GPD parameterization provides a significantly worse description of the magnetic form factor.

Focusing on the very low Q^2 data, we see that G_M^u falls more slowly than the dipole, indicating a magnetic radius smaller than the 0.81 fm associated with the dipole form. The magnitude of the down quark contribution falls more rapidly with Q^2, indicating a larger radius, although because G_M^d is negative this corresponds to an increase in the ratio. The uncertainty on the proton's magnetic radius is significantly larger than for the electron radius [37, 59, 87], so while the magnetization distribution is clearly larger for the down quarks than for the up quarks, opposite of what is observed for the charge radius, it is difficult to determine how these compare to the overall proton magnetization radius.

D. Flavor-dependent contributions to σ_R

Using Eqs. (2) and (7), the reduced cross section in the Born approximation can be written as

$$\sigma_R = \left(\frac{2}{3}G_M^u - \frac{1}{3}G_M^d\right)^2 + \frac{\varepsilon}{\tau}\left(\frac{2}{3}G_E^u - \frac{1}{3}G_E^d\right)^2 \qquad (11)$$

which can be separated into terms coming from just the up-quark or down-quark contributions and the up-down interference term:

$$\begin{aligned}\sigma^{(u)} &= \left(\frac{2}{3}G_M^u\right)^2 + \frac{\varepsilon}{\tau}\left(\frac{2}{3}G_E^u\right)^2,\\ \sigma^{(d)} &= \left(\frac{-1}{3}G_M^d\right)^2 + \frac{\varepsilon}{\tau}\left(\frac{-1}{3}G_E^d\right)^2,\\ \sigma^{(u)\times(d)} &= 2\left(\frac{2}{3}G_M^u\right)\left(\frac{-1}{3}G_M^d\right) + \frac{2\varepsilon}{\tau}\left(\frac{2}{3}G_E^u\right)\left(\frac{-1}{3}G_E^d\right).\end{aligned} \qquad (12)$$

Figure 7 shows the total and flavor-separated contributions to the reduced cross section as a function of ε for a sample of Q^2 values. The down-quark term, $\sigma^{(d)}$ is extremely small, often smaller than the TPE corrections. The up-quark $\sigma^{(u)}$, and the up-down quark interference $\sigma^{(u)\times(d)}$ are the dominant contributions, with the up-down interference term being comparable in size to the total reduced cross section at low Q^2 values. So while down-quark contribution, representing the form factor one would obtain if only the down quark distribution was present, is almost negligible at all values of ε and Q^2, the net impact of the down-quarks on the cross section is still large, especially at low Q^2 values. Note that the strange-quark contributions have been neglected, and while the contributions coming from $(G_{E,M}^s)^2$ will have a negligible contribution to the cross section, the up-strange interference term will be significantly larger, and could have a non-negligible contribution.

To simplify the examination of the flavor-dependent contributions, we examine the contribution of the up, down, and interference terms to $(G_E^p)^2$ and $(G_M^p)^2$, as shown in Fig. 8. For $\varepsilon = 0$, the cross section depends on $(G_M^p)^2$ which is dominated by the up-quark contribution, with a roughly 20% contribution from the interference term adding to $(G_M^p)^2$ at all Q^2 values.

The breakdown of the charge form factor is more complicated. At low Q^2 values, the interference term is roughly half the size of the up-quark contribution and of the opposite sign, making the interference term nearly identical in magnitude to the total value of $(G_E^p)^2$. Increasing from $Q^2 \approx 0.1$ to 1 $(\mathrm{GeV/c})^2$, the decrease in

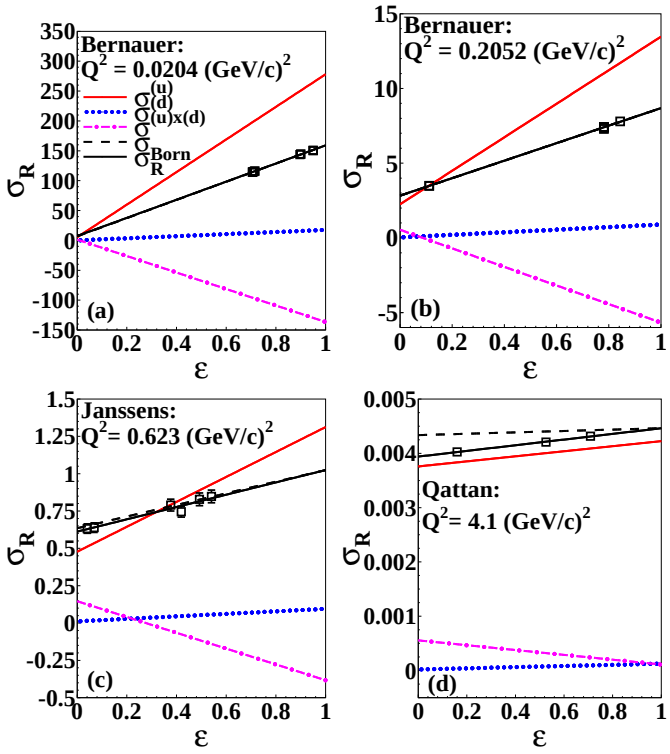

FIG. 7: (Color online) The reduced cross section σ_R including TPE (solid black line) and without TPE (long-dashed black line), along with the flavor-separated contributions to the Born cross section: $\sigma^{(u)}$ (up-quark) (solid red line), $\sigma^{(d)}$ (down-quark) (large-dotted blue line), and $\sigma^{(u)\times(d)}$ (up-down interference) (dashed-dotted magenta line).

G_E^p is driven by the increase in the magnitude of the (negative) up-down interference term, moderated by a slight increase in the up-quark contribution. Above 1-2 $(\mathrm{GeV/c})^2$, the rapid fall of $(G_E^p)^2$, partially cancelled by an increase in both the down-quark and up-down interference terms, continues the very nearly linear decrease observed in the $\mu_p G_E^p/G_M^p$ ratios. Thus, the observed nearly linear behavior comes from a complicated combination of the up, down, and interference terms, with none of the individual contributions showing such a monotonically decreasing behavior relative to the dipole form.

The faster falloff of the down-quark contributions was interpreted in Ref. [10] and references therein as an indication of the possibility of sizable nonzero strange matrix elements at large Q^2 or the importance of diquark degrees of freedom. While existing measurements of parity-violating elastic scattering yield very small contributions from the strange quarks up to $Q^2 \approx 1$ $(\mathrm{GeV/c})^2$ [88–91], they still leave open the possibility for significant contributions from G_E^s and G_M^s which cancel in the parity-violating observables [91, 92], although there are also results from lattice QCD that the strange-quark contribution is small for the charge and magnetic form factors [93, 94].

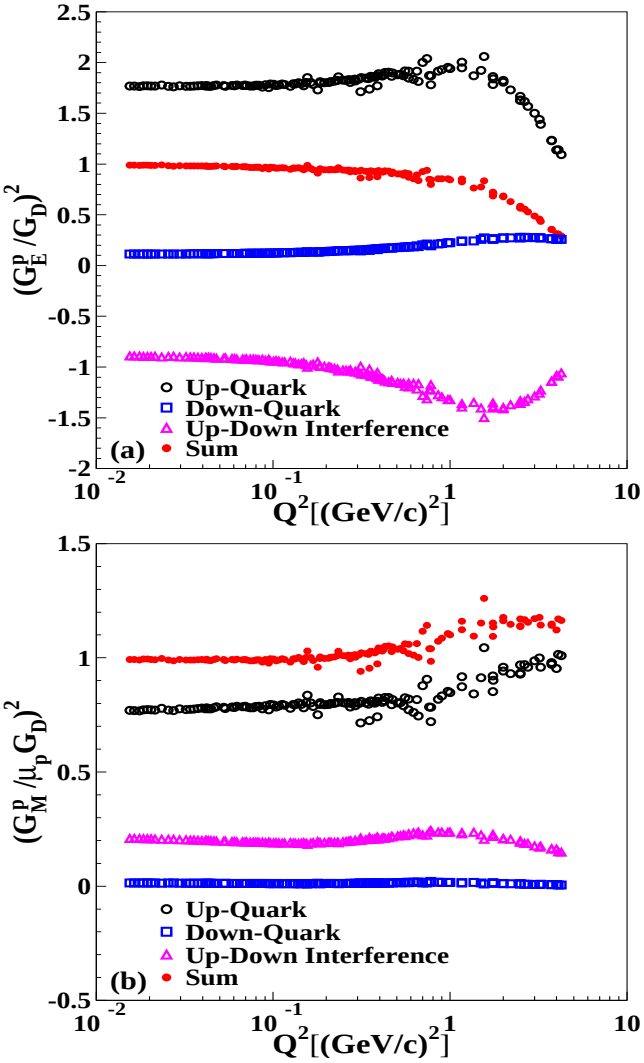

FIG. 8: (Color online) Flavor-separated contributions to $(G_{E,M}^p)^2$: up-quark (open black circles), down-quark (open blue squares), up-down interference (open magenta triangles), and sum (solid red circles).

In the diquark model, the singly occurring down-quark in the proton is more likely to be associated with an axial-vector diquark than a scalar diquark, and the contribution of the axial-vector diquark yields a more rapid falloff of the form factors. The up quarks are generally associated with the more tightly bound scalar diquarks, yielding a harder form factors [10, 81, 82, 85, 95–102]. Recent calculations [99] suggest that pion loop corrections play a crucial rule for $Q^2 \lesssim 1.0$ $(\mathrm{GeV/c})^2$. The nucleon form factors were expressed as proton quark sector form factors, and was found that the down-quark sector of the Dirac form factor is much softer than the up-quark sector as a consequence of the dominance of scalar diquark correlations in the proton wave function. On the other hand, the up-quark sector of the Pauli form factor is slightly softer than in the down-quark sector suggesting that the pion cloud and axial-vector diquark correlations

dominate the effect of scalar diquark correlations leading to a larger down-quark anomalous magnetic moment and a form factor in the up-quark sector that is slightly softer than in the down-quark sector.

IV. CONCLUSIONS

In conclusion, we improved on and extended to lower Q^2 the previous extraction [7] of form factors and two-photon exchange contributions, as well as the extraction [11] of flavor-separated contributions to the proton form factors. We used new polarization data to obtain an improved parameterization of $\mu_p G_E^p/G_M^p$ and its uncertainties, and included new cross section data [37, 43, 59] to extend the analysis to lower Q^2 values.

The results for G_E^p are generally in excellent agreement with those extracted based on a global analysis including calculated TPE hadronic corrections [63, 65], as well as some previous phenomenological extractions [37, 51, 67, 68]. For G_M^p, the results disagree noticeably with previous extractions which applied hadronic TPE corrections and as well as some previous phenomenological extractions. This is in large part due to the tension between the new low-Q^2 Mainz data [37], although the different approaches for applying TPE corrections have some impact as well, especially for extractions which neglected TPE.

Our new low Q^2 extraction of the TPE contribution yields values of $a(Q^2)$ at the few percent level. The TPE term shows a change of sign at $Q^2 \approx 0.40$ (GeV/c)^2, which was not seen in our previous extractions and fit [7], but which is consistent with low Q^2 TPE calculations [20, 21, 32, 41, 103]. This is the first phenomenological extraction that directly observes this predicted change of sign in the comparison of Rosenbluth and polarization data at very low Q^2 values. The change of sign was present in the extraction of Bernauer *et al.* [37], but this was assured by the fact that the high-Q^2 discrepancy requires $a(Q^2) < 0$, while the low Q^2 limit in this extraction was taken to be the Feshbach correction [42], for which $a > 0$. Thus, the combination of the high-Q^2 discrepancy and assumed functional form guarantee the change of sign.

We compared our extracted TPE corrections to previous phenomenological extractions and to world's data on the ratio of positron–proton and electron–proton scattering cross sections, $R_{e^+e^-}$. Our extracted TPE contributions are in generally good agreement with world's data on $R_{e^+e^-}$, including recent measurements which show a clear ε dependence, consistent with the form factor discrepancy, at Q^2 values of 1-1.6 (GeV/c)^2 [8, 9].

Inclusion of the new low-Q^2 polarization and cross section data allows us to examine the slope of the form factor at small Q^2, which is connected to the flavor contributions to the RMS charge and magnetization radii of the proton. While the low Q^2 data do not allow for a precise extraction of these radii, we find that both the up- and down-quark distributions are more localized than the overall charge distribution, with $r_d < r_u < r_p$. For the magnetization distributions, the up-quark contribution has a smaller radius than the down-quark contribution, providing another clear indication that the magnetization distribution does not simply come from the spatial distribution of the quarks.

We also express the reduced cross section σ_R in terms of these flavor-separated from factors to shed light on the contributions of the up-quark, down-quark, and up-down quarks interference terms to the Born cross section σ. The up-quark contribution $\sigma^{(u)}$ dominates at all Q^2 values, while the down-quark contributions $\sigma^{(d)}$, representing the cross section one would observe if scattering from only the down quarks, is typically negligible. The interference term, $\sigma^{(u)\times(d)}$, is negative and can be sizeable. While it is always smaller than the up-quark contribution, it can be comparable in size to the total cross section after the significant cancellation between the interference terms and the up- and down-quark terms.

Acknowledgments

This work was supported by Khalifa University of Science, Technology and Research and by the U. S. Department of Energy, Office of Science, Office of Nuclear Physics, under contract DE-AC02-06CH11357. The third author acknowledges the financial support provided by JUST during his sabbatical leave at the University of Nebraska Omaha, USA.

[1] M. N. Rosenbluth, Phys. Rev. **79**, 615 (1950).
[2] N. Dombey, Rev. Mod. Phys. **41**, 236 (1969).
[3] J. Arrington, C. Roberts, and J. Zanotti, J. Phys. **G34**, S23 (2007).
[4] C. Perdrisat, V. Punjabi, and M. Vanderhaeghen, Prog. Part. Nucl. Phys. **59**, 694 (2007).
[5] C. E. Carlson and M. Vanderhaeghen, Ann. Rev. Nucl. Part. Sci. **57**, 171 (2007).
[6] J. Arrington, P. Blunden, and W. Melnitchouk, Prog.Part.Nucl.Phys. **66**, 782 (2011).
[7] I. A. Qattan, A. Alsaad, and J. Arrington, Phys. Rev. **C84**, 054317 (2011).
[8] D. Adikaram *et al.* (CLAS Collaboration), Phys. Rev. Lett. **114**, 062003 (2015).
[9] I. A. Rachek *et al.*, Phys. Rev. Lett. **114**, 062005 (2015).
[10] G. Cates, C. de Jager, S. Riordan, and B. Wojtsekhowski, Phys. Rev. Lett. **106**, 252003 (2011).
[11] I. A. Qattan and J. Arrington, Phys. Rev. **C86**, 065210 (2012).
[12] G. A. Miller, B. M. K. Nefkens, and I. Slaus, Phys. Rep.

194, 1 (1990).
[13] D. H. Beck, and R. D. McKeown, Ann. Rev. Nucl. Part. Sci. **51**, 189 (2001).
[14] A. I. Akhiezer and M. P. Rekalo, Sov. J. Part. Nucl. **4**, 277 (1974).
[15] R. G. Arnold, C. E. Carlson, and F. Gross, Phys. Rev. **C23**, 363 (1981).
[16] P. A. M. Guichon and M. Vanderhaeghen, Phys. Rev. Lett. **91**, 142303 (2003).
[17] J. Arrington, Phys. Rev. **C68**, 034325 (2003).
[18] J. Arrington, Phys. Rev. **C69**, 022201 (R) (2004).
[19] P. G. Blunden, W. Melnitchouk, and J. A. Tjon, Phys. Rev. Lett. **91**, 142304 (2003).
[20] P. G. Blunden, W. Melnitchouk, and J. A. Tjon, Phys. Rev. **C72**, 034612 (2005).
[21] S. Kondratyuk, P. G. Blunden, W. Melnitchouk, and J. A. Tjon, Phys. Rev. Lett. **95**, 172503 (2005).
[22] Y. C. Chen, A. Afanasev, S. J. Brodsky, C. E. Carlson, and M. Vanderhaeghen, Phys. Rev. Lett. **93**, 122301 (2004).
[23] D. Borisyuk and A. Kobushkin, Phys. Rev. **C74**, 065203 (2006).
[24] D. Borisyuk and A. Kobushkin, Phys. Rev. **C78**, 025208 (2008).
[25] I. A. Qattan, Ph.D. thesis, Northwestern University (2005), arXiv:nucl-ex/0610006.
[26] V. Tvaskis *et al.*, Phys. Rev. **C73**, 025206 (2006).
[27] D. Borisyuk and A. Kobushkin, Phys. Rev. **C76**, 022201 (2007).
[28] Y.-C. Chen, C.-W. Kao, and S.-N. Yang, Phys. Lett. **B652**, 269 (2007).
[29] J. Arrington, Phys. Rev. **C71**, 015202 (2005).
[30] J. Guttmann, N. Kivel, M. Meziane, and M. Vanderhaeghen, Eur. Phys. J. **A47**, 77 (2011).
[31] I. A. Qattan and A. Alsaad, Phys. Rev. **C83**, 054307 (2011), [Erratum-ibid. **C84**, 029905 (2011)].
[32] D. Borisyuk and A. Kobushkin, Phys. Rev. C **75**, 038202 (2007).
[33] M. E. Christy *et al.*, Phys. Rev. **C70**, 015206 (2004).
[34] I. A. Qattan *et al.*, Phys. Rev. Lett. **94**, 142301 (2005).
[35] M. Meziane *et al.*, Phys. Rev. Lett. **106**, 132501 (2011).
[36] M. P. Rekalo and E. Tomasi-Gustafsson, Eur. Phys. J. **A22**, 331 (2004).
[37] J. C. Bernauer *et al.* (A1 Collaboration), Phys. Rev. **C90**, 015206 (2014).
[38] D. Borisyuk and A. Kobushkin, Phys. Rev. **D83**, 057501 (2011).
[39] J. Arrington, Phys. Rev. **C69**, 032201 (R) (2004).
[40] Hai-Qing Zhou and Shin Nan Yang, (2014), arXiv:1407.2711 [nucl-th].
[41] J. Arrington and I. Sick, Phys. Rev. **C70**, 028203 (2004).
[42] W. A. McKinley and H. Feshbach, Phys. Rev. **74**, 1759 (1948).
[43] T. Janssens, R. Hofstadter, E. B. Hughes, and M. R. Yearian, Phys. Rev. **142**, 922 (1965).
[44] L. Andivahis *et al.*, Phys. Rev. **D50**, 5491 (1994).
[45] W. Bartel, F.-W. Büsser, W.-R. Dix, R. Felst, D. Harms, H. Krehbiel, J. McElroy, J. Meyer, and G. Weber, Nucl. Phys. **B58**, 429 (1973).
[46] J. Litt *et al.*, Phys. Lett. **B31**, 40 (1970).
[47] C. Berger, V. Burkert, G. Knop, B. Langenbeck, and K. Rith, Phys. Lett. **B35**, 87 (1971).
[48] R. C. Walker *et al.*, Phys. Rev. **D49**, 5671 (1994).
[49] O. Gayou *et al.*, Phys. Rev. Lett. **88**, 092301 (2002).
[50] O. Gayou *et al.*, Phys. Rev. **C64**, 038202 (2001).
[51] A. J. R. Puckett *et al.*, Phys. Rev. **C85**, 045203 (2012).
[52] V. Punjabi *et al.*, Phys. Rev. **C71**, 055202 (2005), [Erratum-ibid. **C71**, 069902 (2005)].
[53] S. Strauch *et al.*, Phys. Rev. Lett. **91**, 052301 (2003).
[54] A. J. R. Puckett *et al.*, Phys. Rev. Lett. **104**, 242301 (2010).
[55] G. Ron *et al.*, Phys. Rev. **C84**, 055204 (2011).
[56] M. K. Jones *et al.*, Phys. Rev. **C74**, 035201 (2006).
[57] G. MacLachlan *et al.*, Nucl. Phys. **A764**, 261 (2006).
[58] M. Paolone *et al.*, Phys. Rev. Lett. **105**, 072001 (2010).
[59] X. Zhan *et al.*, Phys. Lett. **B705**, 59 (2011).
[60] C. B. Crawford *et al.*, Phys. Rev. Lett. **98**, 052301 (2007).
[61] T. Pospischil *et al.*, Eur. Phys. J. **A12**, 125 (2001).
[62] B. D. Milbrath *et al.*, Phys. Rev. Lett. **80**, 452 (1998), [Erratum-ibid. **82**, 2221 (1999)].
[63] J. Arrington, W. Melnitchouk, and J. A. Tjon, Phys. Rev. **C76**, 035205 (2007).
[64] See Supplemental Material at [to be inserted] for the proton form factors, TPE amplitude $a(Q^2)$, and flavor-separated form factors from this work.
[65] S. Venkat, J. Arrington, G. A. Miller, and X. Zhan, Phys. Rev. **C83**, 015203 (2011).
[66] J. J. Kelly, Phys. Rev. **C70**, 068202 (2004).
[67] Earle L. Lomon, Phys. Rev. **C64**, 035204 (2001).
[68] W. Alberico, S. M. Bilenky, C. Giunti, and K. M. Graczyk, Phys. Rev. **C79**, 065204 (2009).
[69] J. Arrington, J. Phys. **G40**, 115003 (2013).
[70] Krzysztof M. Graczyk, and Cezary Juszczak, J. Phys. **G42**, 034019 (2015).
[71] J. Mar *et al.*, Phys. Rev. Lett. **21**, 482 (1968).
[72] D. Yount and J. Pine, Phys. Rev. **128**, 1842 (1962).
[73] A. Browman, F. Liu, and C. Schaerf, Phys. Rev. **139**, B1079 (1965).
[74] R. L. Anderson *et al.*, Phys. Rev. Lett. **17**, 407 (1966).
[75] R. L. Anderson *et al.*, Phys. Rev. **166**, 1336 (1968).
[76] W. Bartel *et al.*, Phys. Lett. **B25**, 242 (1967).
[77] B. Bouquet *et al.*, Phys. Lett. **B26**, 178 (1968).
[78] M. Moteabbed *et al.*, Phys. Rev. **C88**, 025210 (2013).
[79] Megh Niroula, Ph.D. thesis, Old Dominion University (2010), INSPIRE-1288437.
[80] G. Cassiday *et al.*, Phys. Rev. Lett. **19**, 1191 (1967).
[81] I. C. Cloet, G. Eichmann, B. El-Bennich, T. Klahn, and C. D. Roberts, Few-Body Syst. **46**, 1 (2009).
[82] I. C. Cloet and G. A. Miller, Phys. Rev. **C86**, 015208 (2012).
[83] M. Rohrmoser, Ki-Seok Choi, and Willibald Plessas, (2011), arXiv:1110.3665v2 [hep-ph].
[84] M. Rohrmoser, Ki-Seok Choi, and Willibald Plessas, Acta Phys. Polon. Supp. **6**, 371 (2013).
[85] J. Osvaldo Gonzalez-Hernandez, Simonetta Liuti, Gary R. Goldstein, and Kunal Kathuria, Phys. Rev. **C88**, 065206 (2013).
[86] R. Pohl *et al.*, Nature **466**, 213 (2010).
[87] A. Antognini *et al.*, Science **339**, 417 (2013).
[88] K. A. Aniol *et al.* (HAPPEX Collaboration), Phys. Rev. **C69**, 065501 (2004).
[89] D. S. Armstrong *et al.* (G0 Collaboration), Phys. Rev. Lett. **95**, 092001 (2005).
[90] D. Androic *et al.* (G0 Collaboration), Phys. Rev. Lett. **104**, 012001 (2010).
[91] Z. Ahmed *et al.* (HAPPEX Collaboration), Phys. Rev.

Lett. **108**, 102001 (2012).
[92] D. S. Armstrong and R. D. McKeown, Ann. Rev. Nucl. Part. Sci. **62**, 337 (2012).
[93] K. Paschke, A. Thomas, R. Michaels, and D. Armstrong, J. Phys.: Conf. Ser. **299**, 012003 (2011).
[94] D. B. Leinweber *et al.*, Phys. Rev. Lett. **94**, 212001 (2005).
[95] Ian C. Cloet, Craig. D. Roberts and Anthony W. Thomas, Phys. Rev. Lett. **111**, 101803 (2013).
[96] F. E. Close and A. W. Thomas, Phys. Lett. **B212**, 227 (1988).
[97] I. Cloet, W. Bentz, and Anthony W. Thomas, Phys. Lett. **B621**, 246 (2005).
[98] D. J. Wilson, I. C. Cloet, L. Chang, and C. D. Roberts, Phys. Rev. **C85**, 025205 (2012).
[99] Ian. C. Cloet, Wolfgang Bentz, and Anthony W. Thomas, Phys. Rev. **C90**, 045202 (2014).
[100] Ian. C. Cloet and C. D. Roberts, Prog. Part. Nucl. Phys. **77**, 1 (2014).
[101] Ian. C. Cloet, L. Chang, C. D. Roberts, S. M. Schmidt, and P. C. Tandy, Phys. Rev. Lett. **111**, 092001 (2013).
[102] C. D. Roberts, M. S. Bhagwat, A. Holl, and S. V. Wright, Eur. Phys. J. ST. **140**, 53 (2007).
[103] N. Kivel and M. Vanderhaeghen, Phys. Rev. Lett. **103**, 092004 (2009).